

# Electroluminescence of $\gamma$ -CuBr thin films via vacuum evaporation deposition

A. Cowley<sup>1</sup>, F. Olabanji Lucas<sup>1</sup>, E. Gudimenko<sup>2</sup>, M. M. Alam<sup>1</sup>, D. Danieluk<sup>3</sup>, A. L. Bradley<sup>3</sup> and P.J.

McNally<sup>1</sup>.

1. Nanomaterials Processing Laboratory, Research Institute for Networks and Communications Engineering (RINCE), School of Electronic Engineering, Dublin City University, Dublin 9, Ireland.

2. National Centre for Plasma Science and Technology, School of Electronic Engineering, Dublin City University, Dublin 9, Ireland.

3. Semiconductor Photonics, Physics Department, Trinity College, Dublin 2, Ireland.

E-mail: [cowleya3@mail.dcu.ie](mailto:cowleya3@mail.dcu.ie)

## Abstract

$\gamma$ -CuBr is a I-VII wide bandgap mixed ionic-electronic semiconducting material with light emitting properties suitable for novel UV/blue light applications. Its structural and physical properties allow for vacuum deposition on a variety of substrates and herein we report on the deposition of  $\gamma$ -CuBr on Si and Indium Tin Oxide (ITO) coated glass substrates via vacuum evaporation with controllable film thickness from 100 nm to 500 nm. Temperature dependent Photoluminescence (PL) characteristics of these  $\gamma$ -CuBr films on Si (100) reveals familiar  $Z_f$  and  $I_1$  excitonic features. A Thin Film Electroluminescent Device (TFELD) using a  $\gamma$ -CuBr active layer was fabricated and the room temperature Electroluminescence (EL) was obtained for  $\gamma$ -CuBr for the first time. CuBr features relating to known excitonic ( $Z_f$ , 3.1 eV) emissions were observed as well as a number of previously unknown emissions at 3.81 eV, 3.02 eV, 2.9 eV, 2.75 eV, and 2.1 eV. We speculate on the origins of these peaks and attribute them to the presence of monovalent Cu<sup>+</sup> generated during a.c. excitation.

## 1. Introduction

Optoelectronic devices operating beyond the 3 eV range have drawn considerable interest from researchers

owing to the wealth of enabling devices that are envisioned. UV/blue light emitting diodes (LEDs) and laser diodes (LDs) are of particular interest, and a wide range of materials have been identified as having desirable properties for such devices. The leading materials group for such applications are the III-Nitrides, where GaN and its alloys, with Al and In, are now in commercial production [1]. High brightness UV, blue and green LEDs as well as blue LDs are now commonplace. II-VI compound semiconductors (ZnO, ZnS, ZnSe, etc) continue to progress with proven applications in flat panel displays (FPDs), a.c. driven TFELDs [2] as well as lasing applications [3]

Investigation of the Cuprous Halide (CuHa) family for light emission applications in the UV range has focused on primarily on  $\gamma$ -CuCl and to a lesser degree  $\gamma$ -CuBr, both ionic wide band gap I-VII semiconductors (room temperature band gap 3.395 eV and 3.1 eV, respectively). The early work on CuHa materials was primarily on their nonlinear optical properties [4] resulting from their lack of inversion symmetry – CuCl possesses a large Pockels effect for which CuCl based electro-optic light modulators were envisioned [5]. Fundamental studies on the nature of the CuHa excitonic features have also been carried out [6, 7].

Single crystal ingot-like growth via Bridgman, Czochralski and travelling heater methods [8, 9, 10], with a view towards the study of the aforementioned non-linear effects and excitonic features have been developed. Successful polycrystalline epitaxial deposition of  $\gamma$ -CuCl has been demonstrated via vacuum evaporation [11], RF sputtering [12], as well as some success via LPE [13]. These have all shown the viability of deposition onto existing Si substrate technology as well as onto transparent substrates. Electroluminescence via an applied a.c. voltage has also been demonstrated on CuCl/Si based devices [11], wherein band to band and  $Z_3$  excitonic emission was observed at 3.27eV and 3.21eV, respectively. CuCl nanocrystals have been synthesized and embedded in an organic polymer and EL emission also observed [14].

$\gamma$ -CuBr has been similarly deposited via vacuum evaporation on  $Al_2O_3$  substrates [15] for hot exciton studies. RF sputtering of  $\gamma$ -CuBr on glass, Silicon and Copper substrates for electrochemical sensing has been carried out [16] as well as Molecular Beam Epitaxy (MBE) of  $\gamma$ -CuBr on MgO substrates for fundamental interface

studies. Kondo *et al.* [17] have also shown dramatic improvements in the excitonic PL emission of CuBr films generated by film-substrate chemical reaction of CuCl deposited on KBr substrates, whereby annealing catalyses the reaction. This chemical reaction results in the migration of  $\text{Cu}^+$  and  $\text{K}^+$  ions across the interface and the formation of high quality CuBr crystallites within the KBr crystal, which are attributed with the improved PL relative to previously studied films [15]. A simple electrochemical method for the growth of CuBr on ITO glass through a reduction process involving  $\text{CuBr}_2$  in aqueous solution has also been reported and strong PL observed [18]. Interestingly, previous research did not include the electrical pumping of CuBr for light emitting applications.

One drawback of CuHa is its susceptibility to degradation in ambient atmosphere, quickly degrading into various Cu oxyhalides and assuming a green coloration. Solutions to encapsulate deposited CuCl films have already been identified and tested [19] and should be applicable to CuBr films. The stability of the CuHa family increases from CuCl (least stable), to CuBr and CuI (most stable). The free exciton binding energy of the Cuprous Halides is also of considerable interest, these being 190 meV for CuCl and 108 meV for CuBr. Relative to II-VI and III-Nitrides, this is a promising property for experimentation as an exciton-mediated light emitting mechanism.

While  $\gamma$ -CuCl based EL studies continue, we report on our work regarding  $\gamma$ -CuBr as a blue light emitting material system. The stability of CuBr relative to CuCl could allow for potentially greater application towards the goal of CuHa for blue/UV optoelectronics in conjunction with its excitonic luminescence.

## **2. Experimental**

ITO coated glass substrates were obtained from Sigma Aldrich (15-25 ohm/sq surface resistivity). Prior to any deposition, substrates were cleaned thoroughly via a wet organic cleaning regime. All substrates were degreased in Decon solution and other organic solvents. For Si substrates, the residual oxide layer was removed using a HF etch. Samples were dried using a nitrogen gun before being placed immediately into the vacuum evaporation chamber. Evaporations were carried out within an Edwards 306 system at a pressure of

$1 \times 10^{-6}$  mbar, and growth rates were monitored via an Edwards thin film thickness monitor. Commercially available CuBr powder was supplied from Alfa Aesar (98%). The substrate was at room temperature during deposition. Growth rates of  $\sim 0.3$  nm/s were obtained.

For our temperature dependent measurements, a closed circuit liquid Helium cryostat was used. Laser excitation was at 244 nm, supplied by the frequency doubling of the 488 nm line from an Argon ion laser using a BBO crystal. In conjunction with our temperature dependent measurements, room temperature PL measurements were carried out using a 325 nm UV He-Cd excitation laser. The PL was measured by a liquid Nitrogen cooled CCD detector in conjunction with a 40x UV objective lens, acquired via Horiba Jobin Yvon spectrographic software (LABSPEC 5). X-Ray diffraction (XRD) measurements for this work were acquired using a Bruker AXS D8 Advance x-ray diffractometer. Atomic Force Microscope (AFM) measurements were taken with a Pacific Nanotechnology AFM system. EL measurements were acquired using an OceanOptics 2000 USB spectrometer and UV-fibre optic cable. The spectrometer detector range is from 200 nm to 1100 nm with an optical resolution of  $\sim 0.3$ -10.0 nm FWHM. SiO<sub>2</sub> was deposited by plasma-enhanced chemical vapour deposition (PECVD) technique using hexamethyldisiloxane (HMDSO) and O<sub>2</sub> in a capacitively coupled reactor connected to a 13.56 MHz RF generator. The SiO<sub>2</sub> thickness was determined via ellipsometry measurements and model fitting on a J.A. Woollam XLS-100 ellipsometer. Further details on the growth and characterization of the deposited SiO<sub>2</sub> via PECVD have been reported previously [20].

An illustration of our electroluminescent device structure can be seen in Fig. 1. The ITO substrates had  $\sim 20$  nm of SiO<sub>2</sub> deposited via PECVD prior to the growth of  $\sim 100$  nm  $\gamma$ -CuBr active layer. For the circular contacts on the ELD samples, gold wire from Sigma Aldrich (99.999%) was evaporated using a simple mask. The SiO<sub>2</sub> layer also acts to insulate the ITO from any potential short circuit after Au contacts are deposited via pinholes in the CuBr layer. Contacts to the Au and ITO contacts were made using Gallium-Indium eutectic melt supplied from Sigma Aldrich (99.99%).

### **3. Results and Discussion**

Crystalline and topographical properties of deposited  $\gamma$ -CuBr films were examined with XRD and AFM after evaporation. Figure 2 shows the XRD diffraction pattern for as deposited  $\sim$ 500 nm thin film CuBr on Si (100) substrate. The  $2\theta$  angle of the predominant (111) peak of a  $\gamma$ -CuBr crystal is estimated to be  $27.1^\circ$ , with smaller peaks at  $44.9^\circ$  and  $53.3^\circ$ , in excellent agreement with the powder diffraction standards. The deposited layer is preferentially orientated along the (111)  $\gamma$ -CuBr crystal axis. Some degree of growth along the (220) and (311) orientation can also be seen, but this is minor. This preferential growth is seen within the CuHa family, as previously reported for CuCl vacuum evaporation on Si [11] as well as CuBr growth on  $\text{Al}_2\text{O}_3$  [15]. It should be noted that there was no presence of any wurtzite-phase CuBr that was alluded to in previous work on evaporated CuBr films [21]. AFM surface roughness measurements reveal  $\gamma$ -CuBr films to have a root mean square (RMS) roughness of 7.55 nm. Crystalites can be observed and a general triangular geometry inferred, corresponding to the threefold symmetry of the (111) crystal orientation.

Temperature dependent measurements were taken on various samples ranging from 100-500 nm thickness, which all revealed identical PL spectra. Low temperature PL measurements at 14 K were taken on as-deposited  $\gamma$ -CuBr films of  $\sim$ 500 nm thickness and are presented in Fig 3. Two peaks are clearly evident in the spectrum:  $Z_f$  and  $I_1$  corresponding to the free exciton and impurity bound exciton for CuBr, respectively. In CuBr crystals, the free-exciton PL is attributed to the lowest-energy triplet-exciton state [22]. The bound impurity exciton  $I_1$  is attributed to the  $\text{Cu}^+$  ion vacancies in CuBr [23]. In our temperature dependent PL, the peak intensities for the  $I_1$  and  $Z_f$  can be seen to change with decreasing temperature with the  $I_1$  peak intensity overtaking the free exciton peak intensity near 80-100K. At higher temperatures the  $Z_f$  peak is dominant, in part due to the large excitonic binding energy for CuBr of 108meV. In our films there was no observation of the wide donor-acceptor pair recombination band that was observed in previously evaporated  $\gamma$ -CuBr/ $\text{Al}_2\text{O}_3$  films [24], which attributes a high quality to the deposited  $\gamma$ -CuBr/Si films.

The dominant  $Z_f$  PL peak can be observed in the room temperature spectrum at  $\sim$ 416 nm, which is anomalous considering the well-documented  $Z_f$  peak at 418 nm. However, this can be explained in terms of an increase of the band gap energy related to the increasing temperature. This phenomenon has been previously accounted for in CuCl and is attributed to electron-phonon renormalization of the band gap as

described by Garro and Serrano [25, 26]. Garro *et al.* also claim that this explanation would hold for CuBr. Figure 4 shows the energy of the  $Z_f$  PL peak as a function of temperature. The data clearly shows the increasing energy for the  $Z_f$  exciton PL, with a change from a linear slope around the 80-100 K region. This is in good agreement with Garro's work and confirms that the band gap temperature dependence shown with CuCl films extends to CuBr as well.

Using vacuum evaporation to deposit films of  $\gamma$ -CuBr, we have successfully fabricated a TFELD based on the structure in Figure 1. For our EL measurements, a variable a.c. supply generator with an operating frequency of 50 Hz was used. At voltages of ~4-5 V up to ~16-17 V (peak to peak) we could observe blue light emission. The light was generated from the around the contact area. The emission intensity does tend to dim and flicker but otherwise stays constant. Figure 5 is a typical EL spectrum acquired for these ELDs. A number of peaks are clearly discernible, with the ~418 nm likely corresponding to the  $Z_f$  free exciton emission energy for CuBr. However, the other visible peaks cannot be attributed to known CuBr emission. For a possible explanation of these peaks, we refer to emission studies on copper doped alkali halides and glasses. In these systems, varying emission peaks are observed at similar energies to our own observations, namely at ~320 nm, ~403 nm, ~410 nm, ~450 nm and ~590 nm [27 28, 29]. These emissions are thought to correspond to the  $3d^{10} \mapsto 3d^9 4s$  transitions of the  $Cu^+$  ions present therein.

#### **4. Conclusion**

We have successfully vacuum evaporated  $\gamma$ -CuBr on Silicon and ITO coated glass substrates, observing preferential growth on Si along the (111) crystallographic axis. Using this technique we have successfully fabricated and tested a TFELD using CuBr as an active layer. Characteristic CuBr excitonic peaks as well as possible  $Cu^+$  emissions resulting from an applied potential difference across the device were observed. Room temperature and low temperature measurements also confirm the known excitonic features of  $Z_f$  and  $I_1$ . The ease of deposition of CuBr via vacuum evaporation opens the possibility of deposition of highly crystalline films on a number of potential substrates. The future use of a co-evaporation technique could also allow for the doping of these CuBr films, which could pave the way for a p-n type light emitting CuBr device.

## Acknowledgements

This research was enabled by the Irish Higher Education Authority Program for Research in Third Level Institutions (2007–2011) via the INSPIRE programme. We wish to acknowledge the support of Science Foundation Ireland's Research Frontiers Programme.

## References

- [1] Morkoc H, Strite S, Gao G B, Lin M E, Sverdlov B, Burns M, 1994, *J. Appl. Phys.*, **76**, 1363
- [2] Yi L, Hou Y, Zhao H, He D, Xu Z, Wang Y, Xu X, 2000, *Displays*, **21**, 147
- [3] Haase M, Qui J, DePurdtt K, Cheng H, 1991, *Appl. Phys. Lett.*, **59**, 1272
- [4] Goldmann A, 1977, *Phys. Stat. Sol. (b)*, **81**, 9
- [5] Sterzer F, Blattner D, Minitier S, 1964, *Journal of the Optical Society of America*, **54**, 62
- [6] Andreani L, d'Andrea A, Sole R, 1992, *Phys. Lett. (a)*, **168**, 451
- [7] Goto T, Takahashi T, Ueta M, 1968, *Journal of the Physical Society of Japan*, **24**, 314
- [8] Perner B, 1969, *J. Cryst. Growth*, **6**, 86
- [9] Wilcox W R, Corley R A, 1967, *Material Research Bulletins*, **2**, 571
- [10] Kvapiland J, Perner B, 1971, *J. Cryst. Growth*, **8**, 162
- [11] O'Reilly L, Lucas O, McNally P J, Reader A, 2005, *J. Appl. Phys.*, **98**, 113512
- [12] Natarajan G, 2006, *J. Appl. Phys.*, **100**, 33520
- [13] Cowley A, Foy B, Danilieuk D, McNally P J, 2009, *Phys. Stat. Sol. (a)*, **206**, 923
- [14] Alam M M, Olabanji Lucas F, Danieluk D, Bradley A L, Rajani K V, Daniels S, McNally P J, 2009, *J. Phys. D: Appl. Phys.*, **42**, 225307
- [15] Nakayama M, Soumura A, Hamasaki K, Takeuchi H, Nishimura H, 1997, *Physical Review B*, **55**, 10099
- [16] Seguin J, Bendahan M, Lollmun G, Pasquinelli M, Knauth P, 1998, *Thin Solid Films*, **323**, 31
- [17] Kondo S, Saito T, 2010, *Journal of Luminescence*, **130**, 191
- [18] Li H, Liu R, Kanh H, Zheng Y, Xu Z, 2008, *Electrochimica Acta*, **54**, 242
- [19] Olabanji Lucas F, O'Reilly L, Natarajan G, McNally P J, 2006, *J. Cryst. Growth*, **287**, 112

- [20] Prasad R, Daniels S, Cameron D, McNamara B, Tully E, Kennedy R, 2005, *Surface and Coatings Technology*, **200**, 1031
- [21] Cardona M, 1963, *Physical Review*, **129**, 69
- [22] Ichida H, Nakayama M, Nishimura H, 2000, *Journal of Luminescence*, **87**, 235
- [23] Ueta M, Kanzaki H, 1986, 'Excitonic Processes in Solids' Springer Books
- [24] Kondo S, Mikami K, Saito T, 2008, *Opt. Mater.*, **30**, 1473
- [25] Garro N, Cantarero A, Cardona M, Ruf T, Göbel A, Lin C, Reimann K, Rübenacke S, Steube M, 1996, *Solid State Communications*, **98**, 27
- [26] Serrano J, Schweitzer C, Lin C T, Reimann K, Cardona M, Fröhlich D, 2002, *Physical Review B*, **65**, 125110
- [27] Antonyak O T, Vishnevskii V N, Pidzyrailo N S, Tokarivskii M V, 1974, *Russian Physics Journal*, **17**, 1158
- [28] Wanmaker W L, Spier H L, 1962, *Journal of the Electrochemical Society*, **109**, 109
- [29] Moine B, Pedrini C, Duloisy E, 1991, *J. Phys. IV France*, 1991

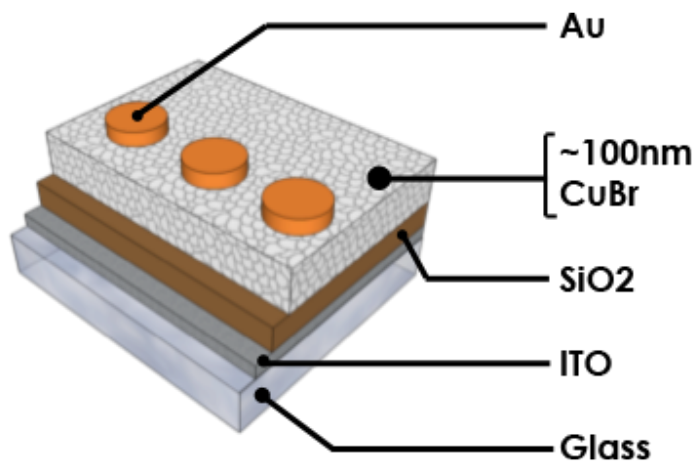


Figure 1 – Cut away illustration detailing layers used in CuBr ELD stack structure.



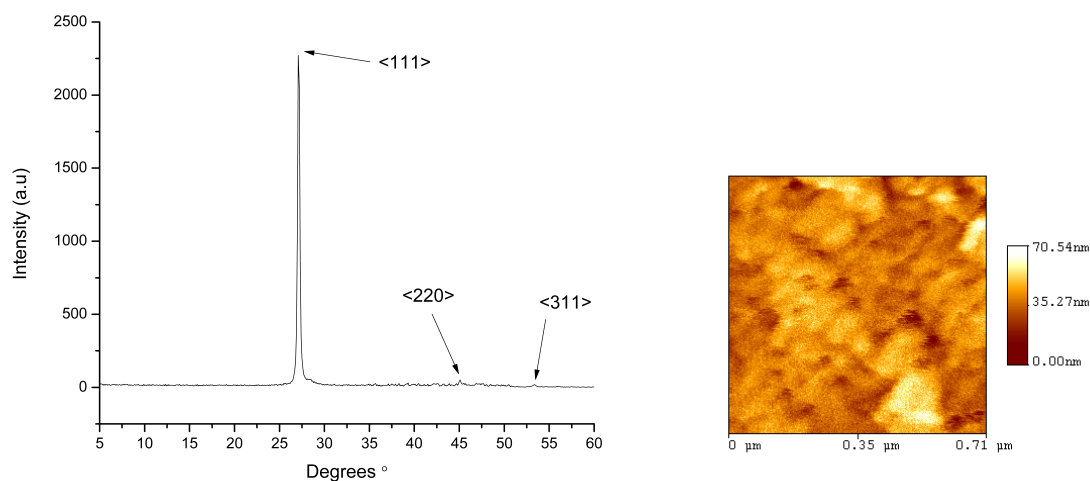


Figure 2 – (a) X-ray  $\theta$ - $2\theta$  diffraction scan for as deposited  $\gamma$ -CuBr & (b) AFM surface image of CuBr layer.

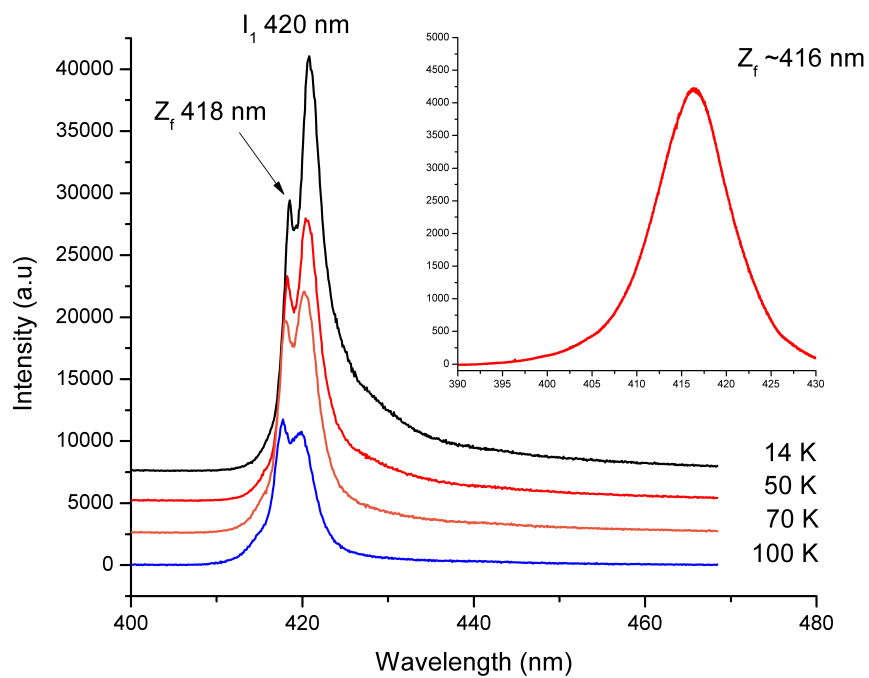


Figure 3 – Temperature dependant PL spectra for  $\gamma$ -CuBr from 14 K to 100 K. Inset corresponding room temperature spectrum.

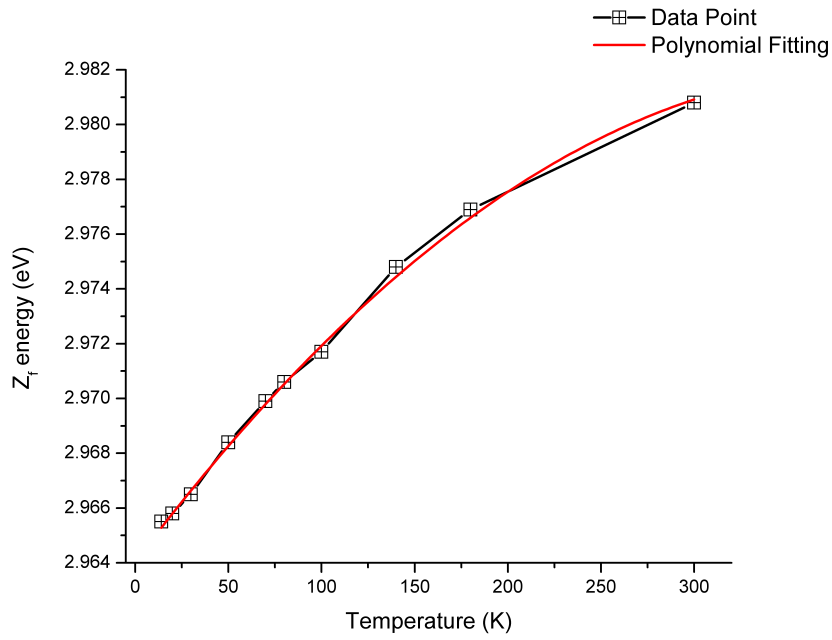


Figure 4 - Variation of free exciton ( $Z_f$ ) energy for  $\sim 500$  nm CuBr thin film on Si(100) as a function of temperature.

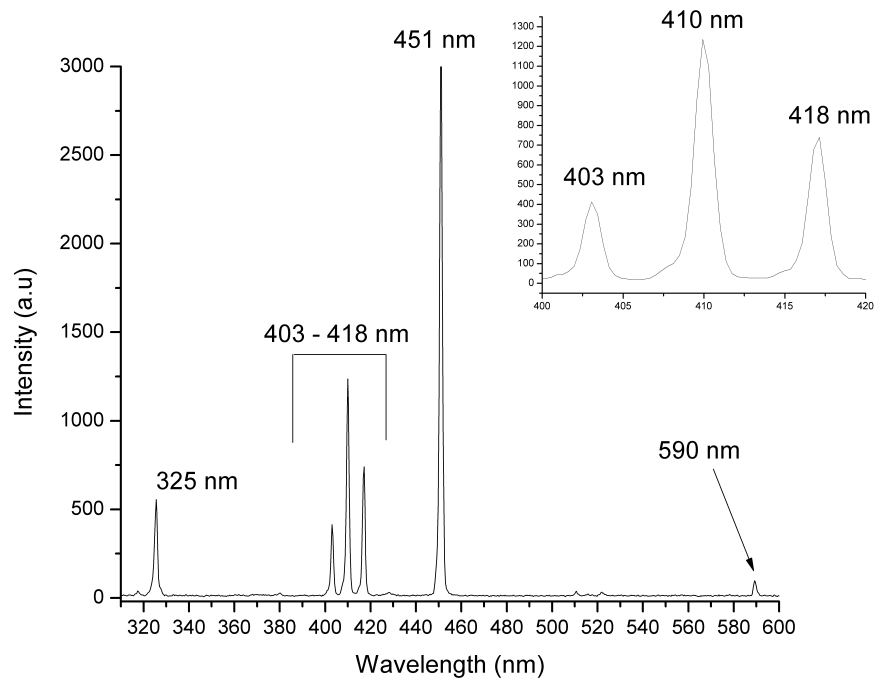


Figure 5 – EL spectrum from device illustrated in Fig. 1 under a.c. excitation, inset showing 400 nm to 420 nm range.